Dielectric antennas - a suitable platform for controlling magnetic dipolar emission

M. K. Schmidt,[1] R. Esteban,[1] J. J. Sáenz,[1,2] I. Suárez-Lacalle,[2] S. Mackowski,[3] and J. Aizpurua[1,*]

[1] *Donostia International Physics Center DIPC and Centro de Física de Materiales CSIC-UPV/EHU, Paseo Manuel de Lardizabal, 5, Donostia-San Sebastián, 20018, Spain*
[2] *Departamento de Física de la Materia Condensada and Instituto Nicolás Cabrera, Universidad Autónoma de Madrid, 28049 Madrid, Spain*
[3] *Optics of Hybrid Nanostructures Group, Institute of Physics, Nicolaus Copernicus University, Grudziadzka 5/7, 87-100 Torun, Poland*
aizpurua@ehu.es

Abstract: Plasmonic nanoparticles are commonly used to tune and direct the radiation from electric dipolar emitters. Less progress has been made towards understanding complementary systems of magnetic nature. However, it has been recently shown that high-index dielectric spheres can act as effective magnetic antennas. Here we explore the concept of coupling dielectric magnetic antennas with either an electric or magnetic dipolar emitter in a similar fashion to the purely electric systems reported previously. We investigate the enhancement of radiation from systems comprising admixtures of these electric and magnetic elements and perform a full study of its dependence on the distance and polarization of the emitter with respect to the antenna. A comparison to the plasmon antennas reveals remarkable symmetries between electric and magnetic systems, which might lead to novel paradigms in the design of nanophotonic devices that involve magnetic activity.

OCIS codes: (250.5403) Plasmonics; (160.3820) Magneto-optical materials; (260.2510) Fluorescence.

References and links

1. E. M. Purcell, "Spontaneous emission probabilities at radio frequencies," Phys. Rev. **69,** 681–681 (1946).
2. M. Ringler, A. Schwemer, M. Wunderlich, A. Nichtl, K. Kürzinger, T. A. Klar, and J. Feldmann, "Shaping emission spectra of fluorescent molecules with single plasmonic nanoresonators," Phys. Rev. Lett. **100,** 203002 (2008).
3. A. Chizhik, F. Schleifenbaum, R. Gutbrod, A. Chizhik, D. Khoptyar, and A. J. Meixner, "Tuning the fluorescence emission spectra of a single molecule with a variable optical subwavelength metal microcavity," Phys. Rev. Lett. **201,** 073002 (2009).
4. S. Kühn, U. Hakanson, L. Rogobete, and V. Sandoghdar, "Enhancement of single-molecule fluorescence using a gold nanoparticle as an optical nanoantenna," Phys. Rev. Lett. **97,** 017402 (2006).
5. P. Anger, P. Bharadwaj, and L. Novotny, "Enhancement and quenching of single-molecule fluorescence," Phys. Rev. Lett. **96,** 113002 (2006).
6. R. Esteban, T. Teperik, and J. Greffet, "Optical patch antennas for single photon emission using surface plasmon resonances," Phys. Rev. Lett. **104,** 026802 (2010).
7. T. H. Taminiau, F. D. Stefani, F. B. Segerink, and N. F. Van Hulst, "Optical antennas direct single-molecule emission," Nat. Photonics **2,** 234–237 (2008).
8. A. G. Curto, G. Volpe, T. H. Taminiau, M. P. Kreuzer, R. Quidant, and N. F. van Hulst, "Unidirectional emission of a quantum dot coupled to a nanoantenna," Science **329,** 930–933 (2010).

#164420 - $15.00 USD Received 8 Mar 2012; revised 19 Apr 2012; accepted 26 Apr 2012; published 4 Jun 2012

9. R. Ruppin, "Decay of an excited molecule near a small metal sphere," J. Chem. Phys. **76,** 1681–1684 (1982).
10. Y. S. Kim, P. T. Leung, and T. F. George, "Classical decay rates for molecules in the presence of a spherical surface: a complete treatment," Surf. Sci. **195**, 1–14 (1988).
11. R. Carminati, J.-J. Greffet, C. Henkel, and J. M. Vigoureux, "Radiative and non-radiative decay of a single molecule close to a metallic nanoparticle," Opt. Commun. **261,** 368–375 (2006).
12. H. Mertens, A. F. Koenderink, and A. Polman, "Plasmon-enhanced luminescence near noble-metal nanospheres: comparison of exact theory and an improved Gersten and Nitzan model," Phys. Rev. B **76**, 115123 (2007).
13. G. Colas des Francs, A. Bouhelier, E. Finot, J. C. Weeber, A. Dereux, C. Girard, and E. Dujardin, "Fluorescence relaxation in the nearfield of a mesoscopic metallic particle: distance dependence and role of plasmon modes," Opt. Express **16,** 17654–17666 (2008).
14. R. J. Glauber and M. Lewenstein, "Quantum optics of dielectric media," Phys. Rev. A **43,** 467–491 (1991).
15. J. P. Dowling and C. M. Bowden, "Atomic emission rates in inhomogeneous media with applications to photonic band structures," Phys. Rev. A **46,** 612–622 (1992).
16. R. D. Artuso, G. W. Bryant, A. Garcia-Etxarri, and J. Aizpurua, "Using local fields to tailor hybrid quantum dot-metal nanoparticle systems: connecting the dots," Phys. Rev. B **83**, 235406 (2011).
17. S. Karaveli and R. Zia, "Spectral tuning by selective enhancement of electric and magnetic dipole emission," Phys. Rev. Lett. **106,** 193004 (2011).
18. A. Alú and N. Engheta, "The quest for magnetic plasmons at optical frequencies," Opt. Express **17,** 5723–5730 (2009).
19. N. Liu, S. Mukherjee, K. Bao, L. V. Brown, J. Dorfmüller, P. Nordlander, and N. J. Halas, "Magnetic plasmon formation and propagation in artificial aromatic molecules," Nano Lett. **12,** 364–369 (2011).
20. A. García-Etxarri, R. Gómez-Medina, L. S. Froufe-Pérez, C. López, L. Chantada, F. Scheffold, J. Aizpurua, M. Nieto-Vesperinas, and J. J. Sáenz, "Strong magnetic response of submicron Silicon particles in the infrared," Opt. Express **19,** 4815–4862 (2011).
21. R. Gómez-Medina, B. García-Cámara, I. Suárez-Lacalle, F. González, F. Moreno, M. Nieto-Vesperinas, and J. J. Sáenz, "Electric and magnetic dipolar response of germanium nanospheres: interference effects, scattering anisotropy, and optical forces," J. Nanophoton. **5,** 053512 (2011).
22. V. V. Klimov and V. S. Letokhov, "Electric and magnetic dipole transitions of an atom in the presence of spherical dielectric interface," Laser Phys. **15,** 61–73 (2005).
23. C. F. Bohren and D. R. Huffman, *Absorption and Scattering of Light by Small Particles* (John Wiley & Sons, 1998).
24. H. C. van de Hulst, *Light Scattering by Small Particles* (Dover, New York, 1981).
25. M. I. Mishchenko, L. D. Travis, and A. A. Lacis, *Scattering, Absorption, and Emission of Light by Small Particles* (Cambridge Univ. Press, 2002).
26. In the absence of absorption, $\Re(a_n) = |a_n|^2$ and $\Re(b_n) = |b_n|^2$, where $\Re(z)$ denotes the real part of z.
27. P. B. Johnson and R. W. Christy, "Optical constants of the noble metals," Phys. Rev. B **6,** 4370–4379 (1972).
28. J. D. Jackson, *Classical Electrodynamics* (Wiley, New York, 1999).

1. Introduction

The idea of controlling the spontaneous decay of a molecule by placing it in an inhomogeneous medium has been extensively investigated since the pioneering work of Purcell [1]. Recent works have been devoted to controlling both the shape [2, 3], intensity [4–6] and directionality [7, 8] of radiation from the dipolar electric emitter by means of coupling the emitter to a variety of metallic antennas.

In a classical description, an electric dipolar transition moment of the molecule is substituted by a dipolar emitter. A classical electrodynamics calculation of the electric fields originated by the dipole allows to calculate the modification of the decay rates, quantum yield and many other properties of the emitter induced by the environment [9–13]. This classical description is known to have a clear correspondence with the quantum results [14–16]. A particularly interesting system with an analytical solution, comprises an electric dipole in the vicinity of a spherical metallic nanoparticle [9], but more complex antenna architectures have also been studied [6–8].

An interesting aspect of dipolar emission is related to the magnetic versus electric nature of the dipolar emitter. Karaveli and Zia [17] have recently shown that, similar to the electric dipolar transition, spontaneous emission from certain molecules exhibiting a magnetic dipolar transition can be modified by carefully placing them near a flat gold mirror. Furthermore, as a growing interest has been given to the various magnetic phenomena occurring in nanoscale

#164420 - $15.00 USD Received 8 Mar 2012; revised 19 Apr 2012; accepted 26 Apr 2012; published 4 Jun 2012

systems [18], such as the excitation of magnetic resonances in metallic [19] and dielectric particles [20–22], a possibility of designing simple platforms for controlling magnetic emission is thus at hand.

In this paper, we demonstrate the possibility of using spherical dielectric nanoparticles as antennas in the optical-infrared range, to modify the radiation from a localized magnetic dipolar emitter. We first present the analytical expressions describing the enhancement of decay rates of an electric dipolar emitter in the vicinity of a spherical nanoparticle and derive the equivalent expressions for the magnetic dipolar emitter. Submicron silicon particles of 230 nm radius are used here as a canonical example of dielectric antennas, since they exhibit spectrally well-separated electric and magnetic dipolar resonances in the near infrared [20]. Interestingly, for both electric and magnetic emitters, we observe a strong dependence of the excitations on the orientation of the emitter with respect to the surface of the antenna. This setup is then compared to a more familiar system where an electric dipolar emitter is placed near a small plasmonic nanoparticle acting as an optical electric nanoantenna. Finally, we show that a simple dipole-dipole interaction model allows to describe in a simplified manner the enhancement of emission rates in several relevant situations.

2. Electric and magnetic dipolar decay rates in the presence of a particle

Recent developments in the understanding and engineering of magnetic phenomena in nano-optics call for analytical methods to describe the properties of their building blocks. An example of that is the enhancement of the radiation rate from a magnetic dipole placed in an inhomogeneous environment. The analytical formulas describing the enhancement of radiative and non-radiative decay rates of an electric dipole positioned in the vicinity of a spherical nanoparticle have been derived by Ruppin [9]. Following this work, we derive analogous expressions for the magnetic dipole. First, the dipolar electromagnetic field is expanded into a series of vector spherical harmonics, and the response from the sphere to each harmonic is obtained following the Mie formalism [23–25]. Integrating the flow of Poynting vector through the full solid angle in the far-field gives the radiated power. The ohmic losses associated with induced currents within the particle give the rate of energy dissipation. The sum of the radiative decay rate Γ_{RAD} and the non-radiative decay rate $\Gamma_{NON-RAD}$ gives the total decay rate Γ_{TOT}. The detailed derivation is presented in the Appendix.

Below, we list the expressions for the radiative and total decay rates enhancements of the electric (superscript 'e') and magnetic ('m') dipoles. Two orientations of the emitter are considered and denoted with superscripts in the decay rates: perpendicular ('$\perp$') and parallel ('$||$') to the closest surface of the spherical antenna. The dipole is positioned at the distance z from the center of a homogeneous sphere of radius a and dielectric constant ε. The system is embedded in an environment characterized by the real-valued dielectric function ε_e. The wavevector $k = 2\pi/\lambda\sqrt{\varepsilon_e}$ is associated with the vacuum radiation wavelength of the emitter λ. The decay rates are normalized to the decay rate of the dipole in the homogeneous environment Γ_0. Within the linear response theory, the obtained enhancement factors are independent of the strength of the emitter and are given by

$$\frac{\Gamma_{RAD}^{\perp,e}}{\Gamma_0} = \frac{3}{2}\sum_{n=0}^{\infty}(2n+1)n(n+1)\left|\frac{j_n(kz) - a_n h_n^{(1)}(kz)}{kz}\right|^2 \tag{1}$$

$$\frac{\Gamma_{TOT}^{\perp,e}}{\Gamma_0} = 1 - \frac{3}{2}\Re\sum_{n=0}^{\infty}(2n+1)n(n+1)a_n\left[\frac{h_n^{(1)}(kz)}{kz}\right]^2 \tag{2}$$

#164420 - $15.00 USD Received 8 Mar 2012; revised 19 Apr 2012; accepted 26 Apr 2012; published 4 Jun 2012

$$\frac{\Gamma_{RAD}^{||,e}}{\Gamma_0} = \frac{3}{4}\sum_{n=0}^{\infty}(2n+1)\left[|j_n(kz) - b_n h_n^{(1)}(kz)|^2 + \left|\frac{\psi_n'(kz) - a_n\zeta_n'(kz)}{kz}\right|^2\right]^2 \tag{3}$$

$$\frac{\Gamma_{TOT}^{||,e}}{\Gamma_0} = 1 - \frac{3}{4}\sum_{n=0}^{\infty}(2n+1)\Re\left[a_n\left[\frac{\zeta_n'(kz)}{kz}\right]^2 + b_n[h_n^{(1)}(kz)]^2\right] \tag{4}$$

where $\Re(z)$ denotes the real part of z.
For the magnetic emitter, the respective enhancement factors are given by (see Appendix for a detailed derivation)

$$\frac{\Gamma_{RAD}^{\perp,m}}{\Gamma_0} = \frac{3}{2}\sum_{n=0}^{\infty}(2n+1)n(n+1)\left|\frac{j_n(kz) - b_n h_n^{(1)}(kz)}{kz}\right|^2 \tag{5}$$

$$\frac{\Gamma_{TOT}^{\perp,m}}{\Gamma_0} = 1 - \frac{3}{2}\Re\sum_{n=0}^{\infty}(2n+1)n(n+1)b_n\left[\frac{h_n^{(1)}(kz)}{kz}\right]^2 \tag{6}$$

$$\frac{\Gamma_{RAD}^{||,m}}{\Gamma_0} = \frac{3}{4}\sum_{n=0}^{\infty}(2n+1)\left[|j_n(kz) - a_n h_n^{(1)}(kz)|^2 + \left|\frac{\psi_n'(kz) - b_n\zeta_n'(kz)}{kz}\right|^2\right]^2 \tag{7}$$

$$\frac{\Gamma_{TOT}^{||,m}}{\Gamma_0} = 1 - \frac{3}{4}\sum_{n=0}^{\infty}(2n+1)\Re\left[b_n\left[\frac{\zeta_n'(kz)}{kz}\right]^2 + a_n[h_n^{(1)}(kz)]^2\right]. \tag{8}$$

Bessel-Ricatti functions ψ and ζ are defined as $\psi(x) = xj_n(x)$ and $\zeta(x) = xh_n^{(1)}(x)$ with the use of spherical Bessel $j_n(x)$ and Hankel functions $h_n^{(1)}(x)$ of the first kind. The definitions of Mie coefficients a_n and b_n used here are adopted from Bohren and Huffman [23]:

$$a_n = \frac{M\psi_n(k_1a)\psi_n'(ka) - \psi_n(ka)\psi_n'(k_1a)}{M\psi_n(k_1a)\zeta_n'(ka) - \zeta_n(ka)\psi_n'(k_1a)} \tag{9}$$

$$b_n = \frac{\psi_n(k_1a)\psi_n'(ka) - M\psi_n(ka)\psi_n'(k_1a)}{\psi_n(k_1a)\zeta_n'(ka) - M\zeta_n(ka)\psi_n'(k_1a)} \tag{10}$$

with $k_1 = k\sqrt{\varepsilon/\varepsilon_e} = kM$, where M is defined as the relative refractive index. In all the following considerations, we will assume a vacuum environment characterized by $\varepsilon_e = 1$. All the derivatives in the above expressions are calculated with respect to the arguments in parentheses. The Mie coefficients can be attributed to the efficiency of excitation of the corresponding electric (a_n) and magnetic (b_n) Mie modes. The first two Mie resonances $n = 1,2$ correspond to the dipolar and quadrupolar modes, respectively. Notably, the expressions for the decay of an electric emitter (Eqs. (1)-(4)) differ from those for the magnetic emitter (Eqs. (5)-(8)). It is possible to relate one with another by exchanging the Mie coefficients $a_n \leftrightarrow b_n$ [22]. Furthermore, in the absence of absorption (real $\sqrt{\varepsilon}$), the enhancements of total and radiative decay rates can be shown to be equal, using the properties of the Mie coefficients [26].

3. Radiating dipoles in the presence of a high-index dielectric particle (Si sphere)

It has been previously shown that a high-permittivity sub-micron size nanoparticle can exhibit strong and spectrally separated electric and magnetic dipolar resonances in the near-infrared [20]. In Fig. 1(a) we show the normalized plane wave scattering cross section spectrum of a silicon sphere of radius $a = 230$ nm (relative refractive index $M = 3.5$), separated into dominant dipolar ($n = 1$) and quadrupolar ($n = 2$) contributions. The scattering cross section under plane

#164420 - $15.00 USD Received 8 Mar 2012; revised 19 Apr 2012; accepted 26 Apr 2012; published 4 Jun 2012

wave illumination (Fig. 1(b)) can be decomposed into electric ($\sigma_s(a_n)$) and magnetic ($\sigma_s(b_n)$) contributions according to

$$\sigma_s = \frac{2\pi}{k^2}\sum_{n=1}^{\infty}(2n+1)(\Re(a_n)+\Re(b_n)) = \sum_{n=1}^{\infty}(\sigma_s(a_n)+\sigma_s(b_n)) \tag{11}$$

Spectra in Fig. 1(a) show the scattering efficiency of the nanoparticle defined as the scattering cross section normalized by the geometrical cross section $C_s = \sigma_s/(\pi a^2)$. In the investigated range of wavelengths, three peaks at $\lambda = 1160$ nm, $\lambda = 1350$ nm and $\lambda = 1680$ nm can be identified and attributed to, respectively, the quadrupolar magnetic b_2, the dipolar electric a_1 and the dipolar magnetic b_1 resonances.

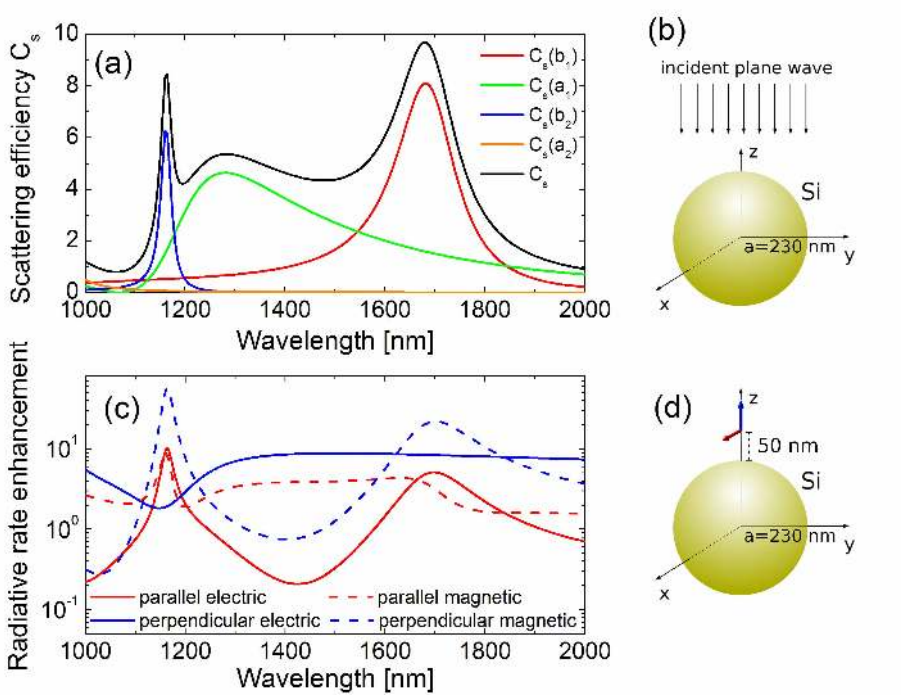

Fig. 1. Spectral features of the scattering cross section of a 230 nm radius Si nanosphere in vacuum illuminated by a plane wave (a) and the decay rate enhancements of an electric or magnetic emitter positioned in the vicinity of the particle (c). The schematics of the systems are shown in (b) and (d), respectively. In (a), the total scattering efficiency C_s is separated into different contributions: electric (a_1) and magnetic dipolar (b_1), electric (a_2) and magnetic quadrupolar (b_2), according to Eq. (11). Spectra of the radiative rate enhancements shown in (c) were calculated using Eqs. (2),(4),(6),(8) for the electric (solid lines) and magnetic (dashed lines) emitter. The emitter is oriented either perpendicularly (blue lines) or parallelly (red lines) with respect to the closest surface of the sphere. The refractive index of the silicon nanosphere is 3.5, while the distance from the emitter to the surface of the sphere is set to 50 nm.

In Fig. 1(c), we present the spectra of the enhancement of the decay rates for both electric and magnetic emitters positioned at 50 nm distance from the surface of the silicon sphere (Fig. 1(d)). The enhancements for electric (solid lines) and magnetic (dashed lines) dipoles are shown for the two orientations of both types of emitters - parallel (red lines) and perpendicular (blue lines) to the closest surface of the nanoparticle (see schematics in Fig. 1(d)). For each configuration,

#164420 - $15.00 USD Received 8 Mar 2012; revised 19 Apr 2012; accepted 26 Apr 2012; published 4 Jun 2012

modes excited by the emitter can be identified by the correspondence between the spectral positions of the peaks in the decay rate enhancement spectra in Fig. 1(c) and the maxima of Mie coefficients in Fig. 1(a).

We observe in Fig. 1(c) that both the orientation of the emitters as well as their electric or magnetic nature determine which modes of the sphere are excited. An electric emitter oriented parallelly (solid red line) excites the magnetic dipolar b_1 (at $\lambda = 1680$ nm), quadrupolar b_2 (at $\lambda = 1160$ nm) and - although very weakly - the electric dipolar a_1 (at $\lambda = 1350$ nm) resonance, while the same emitter aligned perpendicularly (solid blue line) couples only to the broad electric dipolar a_1 mode at $\lambda = 1350$ nm. The complementary behavior is present for the magnetic emitter: for the perpendicular orientation (blue dashed line), only the magnetic b_1, b_2 modes are excited, while in the parallel orientation (red dashed line) the emitter couples to both the magnetic and electric modes. In principle, this effect can thus be used to discriminate between the two types of emitters.

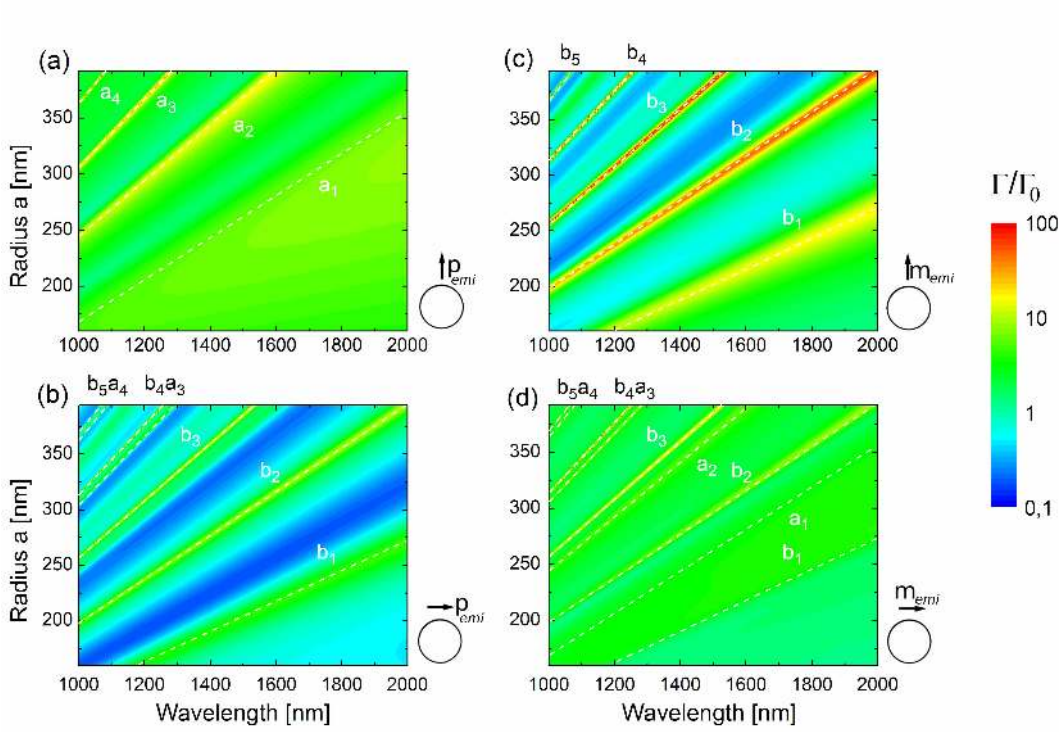

Fig. 2. Spectra of the decay rate enhancements of electric ($\mathbf{p}_{emi}$, (a,b)) or magnetic ($\mathbf{m}_{emi}$, (c,d)) nature near the silicon sphere of varying radius a in vacuum. Dipoles are oriented either perpendicularly (a,c) or parallelly (b,d) to the surface of the antenna, positioned at the fixed distance of 50 nm from its surface. Dashed lines correspond to the Mie resonances a_n and b_n, as denoted in each of the plots. Geometries of the setup are shown in the schematics.

To further investigate the selectivity of the emission, we plot in Fig. 2 the enhancements of the decay rates of the electric ($\mathbf{p}_{emi}$) and magnetic ($\mathbf{m}_{emi}$) dipolar emitter as a function of the radiation wavelength λ and the radius a of the dielectric nanosphere. Since Eqs. (1)-(10) depend on the parameter ka through the Mie coefficients, spectral positions of the Mie resonances form straight lines as marked in the maps in Fig. 2 by dashed lines defined by $a \propto \lambda$. The dependence of Eqs. (1)-(10) on the distance from the dipole to the center of the sphere z does not affect

#164420 - $15.00 USD Received 8 Mar 2012; revised 19 Apr 2012; accepted 26 Apr 2012; published 4 Jun 2012

significantly the spectral features of the enhancements, but governs the relative strength of the resonances. Furthermore, for the largest sphere, many high-order resonances appear clearly in the high-energy region of spectra, as these modes can be efficiently activated for small values of $(z-a)/a$.

Similarly to Fig. 1(c), for perpendicular orientation, the electric emitter (Fig. 2(a)) couples only to the electric modes (marked as a_n), and excites mostly magnetic contribution when oriented parallelly (Fig. 2(b)). In the latter case however, an electric contribution is also present, which is mostly visible for the high order modes. Similarly, the perpendicular magnetic emitter excites magnetic modes exclusively (Fig. 2(c)), whereas in parallel orientation it couples to the electric and to the magnetic modes (Fig. 2(d)). Thus, the orientation and nature of the emitters allows to select which modes of the dielectric sphere are excited.

This modal selectivity can be understood by tracing the presence of Mie coefficients in Eqs. (1)-(8) for each case. For the emitter perpendicular to the surface of the antenna (Eqs. (1),(2),(5),(6)), only one type of Mie coefficients is present: electric a_n terms for the electric emitter and magnetic b_n terms for the magnetic emitter. On the other hand, the equations for the emitter oriented parallelly (Eqs. (3),(4),(7),(8)) include both electric and magnetic coefficients, therefore both types of resonances are excited. These properties reflect the symmetry of Eqs. (1)-(4) and Eqs. (5)-(8) with respect to the exchange of the electric and magnetic Mie coefficients in the sums.

So far, we have identified the peaks in Fig. 1 and Fig. 2 by studying different contributions to the sum in Eq. (11). This identification can be confirmed by plotting the distributions of the fields induced in each case. In Fig. 3 the induced electric (a,c,e,g) and magnetic field (b,d,f,h) distributions are shown for two resonances of the Si sphere - electric a_1 ((a-d), denoted in the schematics as $\mathbf{p}_{ind}$) and magnetic b_1 ((e-h), $\mathbf{m}_{ind}$) dipolar modes. The excitations are due to the emitter of the electric ($\mathbf{p}_{emi}$) or magnetic ($\mathbf{m}_{emi}$) nature, oriented as shown in the schematic of Fig. 3. The fields have been obtained from a vector harmonic decomposition (see Appendix for details). Dipolar electric resonances at $\lambda = 1350$ nm are excited by the perpendicularly oriented electric emitter (Fig. 3(a), 3(b)) or parallelly oriented magnetic emitter (Fig. 3(c), 3(d)). The dipolar magnetic resonance at $\lambda = 1680$ nm is induced both by the electric emitter oriented parallelly (Fig. 3(e), 3(f)) and by the magnetic emitter oriented perpendicularly (Fig. 3(g), 3(h)) to the surface of the sphere. The distributions of the fields shown in Fig. 3 clearly indicate the dipolar nature of the induced resonances and qualitatively agree well with the field distributions at the resonances obtained with excitation of the Si sphere by a plane wave [20].

4. Magnetic emitter in the vicinity of a plasmonic nanoparticle

Small metallic spherical nanoparticles do not exhibit significant magnetic resonances in the visible spectral range, but they present strong plasmonic resonances of electric nature that have been shown to strongly modify the decay rates of nearby electric dipolar emitters. In this section, we demonstrate that the plasmonic mode also affects the emission from a magnetic emitter.

In Fig. 4(a) we show the scattering efficiency spectra of a silver spherical 50 nm radius nanoparticle illuminated by a plane wave (Fig. 4(b)). The decomposition of the scattering efficiency into different contributions, as previously introduced for the silicon sphere in Fig. 1(a), indicates that the scattering properties of the nanoparticle are due to the excitation of the dipolar electric a_1 mode with a broad maximum at around $\lambda \approx 430$ nm.

The spectral dependence of the radiative and total decay rate enhancements in this situation is shown in Fig. 4(c) and Fig. 4(d), respectively. The radiative behavior of the electric (solid line) and magnetic (dashed line) dipoles resembles the features observed in a dielectric sphere: both the perpendicular electric (blue solid line) and parallel magnetic (red dashed line) emitters couple well to an electric a_1 mode, while the parallel electric emitter (red solid line) couples

#164420 - $15.00 USD Received 8 Mar 2012; revised 19 Apr 2012; accepted 26 Apr 2012; published 4 Jun 2012

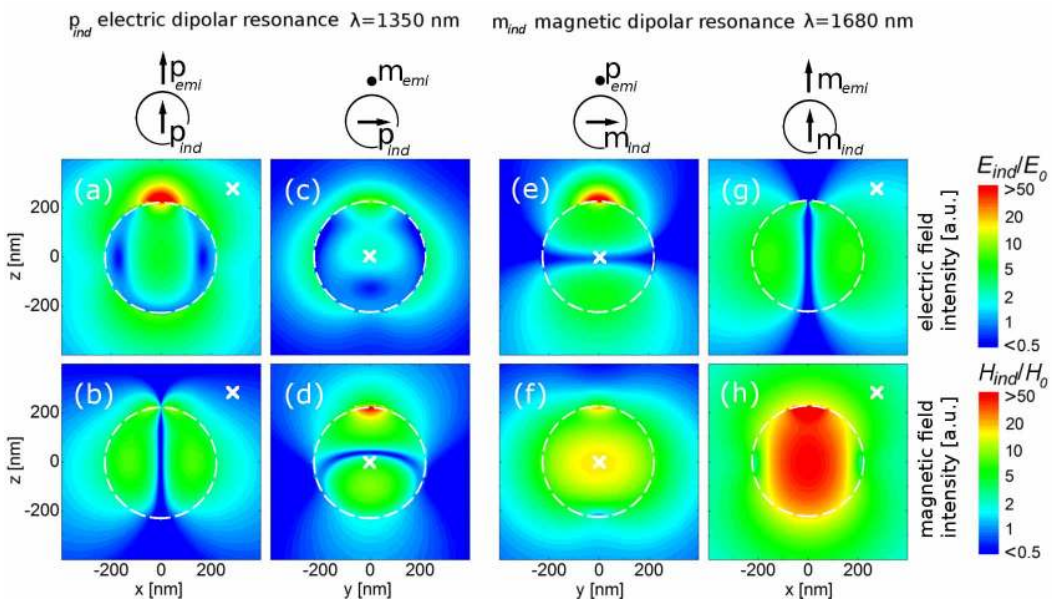

Fig. 3. Distribution of the electric (upper row) and magnetic (lower row) induced field amplitudes by an electric ($\mathbf{p}_{emi}$) and magnetic ($\mathbf{m}_{emi}$) dipole at the 50 nm distance from the surface of a 230 nm radius silicon sphere. Shown cross-sections contain the dipole and the center of the sphere. Plots (a-d) correspond to the dipolar electric mode at $\lambda = 1350$ nm, with the induced dipole denoted as $\mathbf{p}_{ind}$, excited by the perpendicular electric (a,b) or parallel magnetic (c,d) emitter. (e-h) illustrate the field distributions at the dipolar magnetic mode $\lambda = 1680$ nm ($\mathbf{m}_{ind}$), induced by the parallel electric (e,f) or perpendicular magnetic (g,h) emitter. Schematics of the exciting and induced dipoles are shown at the top of the figure. Intensities of the induced fields E_{ind} and H_{ind} are normalized to the values of the fields E_0 and H_0 produced by the dipolar emitter in the absence of the particle and evaluated at the distance of 280 nm from the emitter in the direction perpendicular to its axis. The position of the normalization point is marked by a white cross in each case.

also to the magnetic b_1 mode. The radiation enhancement in the latter case is much weaker because magnetic modes in plasmonic structures are strongly damped. The enhancement of the total decay rate (Fig. 4(d)) is dominated by coupling to higher order modes. These modes are very weakly radiative, but can couple to the dipolar emitter [12] and lead to efficient non-radiative decay. Nevertheless, the excitation of the dipolar electric and magnetic modes exhibits analogous dependence on the orientation and nature of the dipolar emitter as observed for the enhancement of the radiative rates. This suggests that, although the performance of the silicon antennas presented here is better than that of their metallic counterparts to control the emission from magnetic emitters, plasmonic antennas could be also considered as appropriate building blocks to this end.

5. Dipole-dipole interaction

The coupling in the previous examples was often dominated by dipolar modes induced in the sphere. It is convenient to study in more detail the distance dependence of the total decay rate. By limiting the sum in Eqs. (1)-(8) to the $n = 1$ terms and taking the explicit form of the spherical Hankel function $h_1^{(1)}$, we obtain the following expressions for the enhancement of the

#164420 - $15.00 USD Received 8 Mar 2012; revised 19 Apr 2012; accepted 26 Apr 2012; published 4 Jun 2012

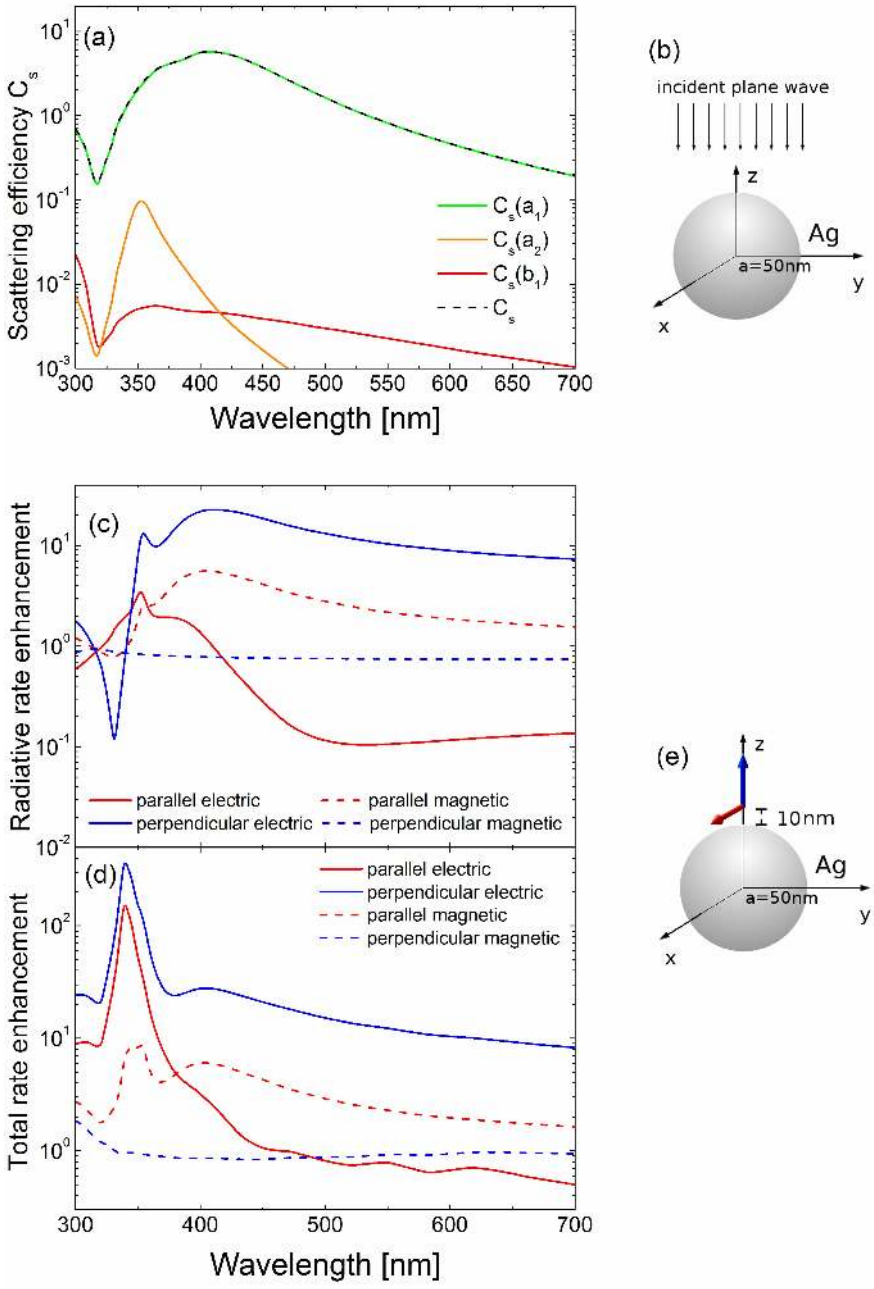

Fig. 4. Spectral features of the scattering efficiency of a 50 nm radius silver nanosphere in vacuum illuminated by a plane wave (a) and the radiative (c) and total (d) decay rate enhancements of an electric and magnetic emitter positioned in the vicinity of the particle. The geometries of the systems for calculating the plane wave extinction and the properties of dipolar emission are depicted in (b) and (e), respectively. In (a), the total scattering efficiency C_s is split into different contributions: electric dipolar (a_1), magnetic dipolar (b_1), electric quadrupolar (b_2), according to Eq. (11). In plots (c) and (d), the enhancement factors of the, respectively, radiative and total decay rates of the dipoles are shown. In both plots, the spectra were calculated for the electric (solid lines) and magnetic (dashed lines) emitters. The orientation of the emitter with respect to the surface of the sphere is either perpendicular (blue lines) or parallel (red lines). The refractive index of the uniform silver nanosphere is taken from [27].

#164420 - $15.00 USD Received 8 Mar 2012; revised 19 Apr 2012; accepted 26 Apr 2012; published 4 Jun 2012

decay rates within the dipole-dipole approximation:

$$\left.\frac{\Gamma_{TOT}^{\perp,e}}{\Gamma_0}\right|_{\text{dip}} = 1+\frac{3k^3}{2\pi}\Im\left[\alpha_E e^{2ikz}\left(-1-\frac{2i}{kz}+\frac{1}{(kz)^2}\right)\right] \tag{12}$$

$$\begin{aligned}\left.\frac{\Gamma_{TOT}^{||,e}}{\Gamma_0}\right|_{\text{dip}} &= 1+\frac{3k^3}{8\pi}\Im\left[\alpha_E e^{2ikz}\frac{1}{(kz)^2}\left(1+\frac{2i}{kz}-\frac{3}{(kz)^2}-\frac{2i}{(kz)^3}+\frac{1}{(kz)^4}\right)\right]\\ &+\frac{3k^3}{8\pi}\Im\left[\alpha_M e^{2ikz}\frac{1}{(kz)^2}\left(-1-\frac{2i}{kz}+\frac{1}{(kz)^2}\right)\right]\end{aligned} \tag{13}$$

$$\left.\frac{\Gamma_{TOT}^{\perp,m}}{\Gamma_0}\right|_{\text{dip}} = 1+\frac{3k^3}{2\pi}\Im\left[\alpha_M e^{2ikz}\left(-1-\frac{2i}{kz}+\frac{1}{(kz)^2}\right)\right] \tag{14}$$

$$\begin{aligned}\left.\frac{\Gamma_{TOT}^{||,m}}{\Gamma_0}\right|_{\text{dip}} &= 1+\frac{3k^3}{8\pi}\Im\left[\alpha_M e^{2ikz}\frac{1}{(kz)^2}\left(1+\frac{2i}{kz}-\frac{3}{(kz)^2}-\frac{2i}{(kz)^3}+\frac{1}{(kz)^4}\right)\right]\\ &+\frac{3k^3}{8\pi}\Im\left[\alpha_E e^{2ikz}\frac{1}{(kz)^2}\left(-1-\frac{2i}{kz}+\frac{1}{(kz)^2}\right)\right],\end{aligned} \tag{15}$$

where the electric α_E and the magnetic α_M dipolar polarizabilities are associated with the first order Mie coefficients according to $\alpha_E = ik^3/(6\pi)a_1$ and $\alpha_M = ik^3/(6\pi)b_1$, respectively. $\Im(z)$ denotes the imaginary part of z.

As in the exact formulas Eqs. (3),(4),(7),(8), only Eqs. (13) and (15) depend on both magnetic (α_M) and electric (α_E) contributions. The perpendicular electric (magnetic) emitter couples only with the electric (magnetic) dipolar mode. In the cases when a single dipolar mode of the sphere, either electric or magnetic, dominates the response at a given wavelength, it is possible to describe the coupling at that wavelength as a simple dipole-dipole interaction.

To illustrate this situation, we show in Fig. 5 the enhancement of the decay rate as a function of the distance between the dipole and the center of the nanoparticle. Results were obtained with the use of the exact formulas given by Eqs. (1)-(8) (solid black lines) as well as with the dipolar-interaction approximation (dashed red lines). We consider the 230 nm radius silicon and the 50 nm silver sphere as in the previous cases. To extract the dominant contributions, we choose the wavelengths corresponding to the dipolar electric a_1 and dipolar magnetic b_1 resonances, and set the polarizabilities of the complementary nature to 0 in Eqs. (12)-(15). Namely, in the case of the Si sphere, α_E is neglected for $\lambda = 1680$ nm (corresponding to b_1 resonance) and α_M is ignored for $\lambda = 1350$ nm (a_1). For the Ag sphere, we put the magnetic dipolar polarizability $\alpha_M = 0$ for $\lambda = 430$ nm (coinciding with the electric dipolar resonance a_1).

The dipole-dipole interaction model very accurately reproduces the exact results in all considered cases. In Fig. 5(a), we plot the decay rate enhancements of an electric emitter, perpendicular to the surface of the silicon sphere, radiating at $\lambda = 1350$ nm (dipolar electric antenna resonance). The disagreement between the curves can be attributed to the influence of the quadrupolar electric mode, not considered in the dipole-dipole approximation. In the analogous situation of an identically oriented magnetic emitter at the magnetic dipolar resonance ($\lambda = 1680$ nm, Fig. 5(d)), the agreement with the analytical solution is almost perfect, as no higher order magnetic modes contribute in this spectral range. Small differences due to the neglected dipolar polarizabilities can be seen for emitters oriented parallelly to the surface of

#164420 - $15.00 USD Received 8 Mar 2012; revised 19 Apr 2012; accepted 26 Apr 2012; published 4 Jun 2012

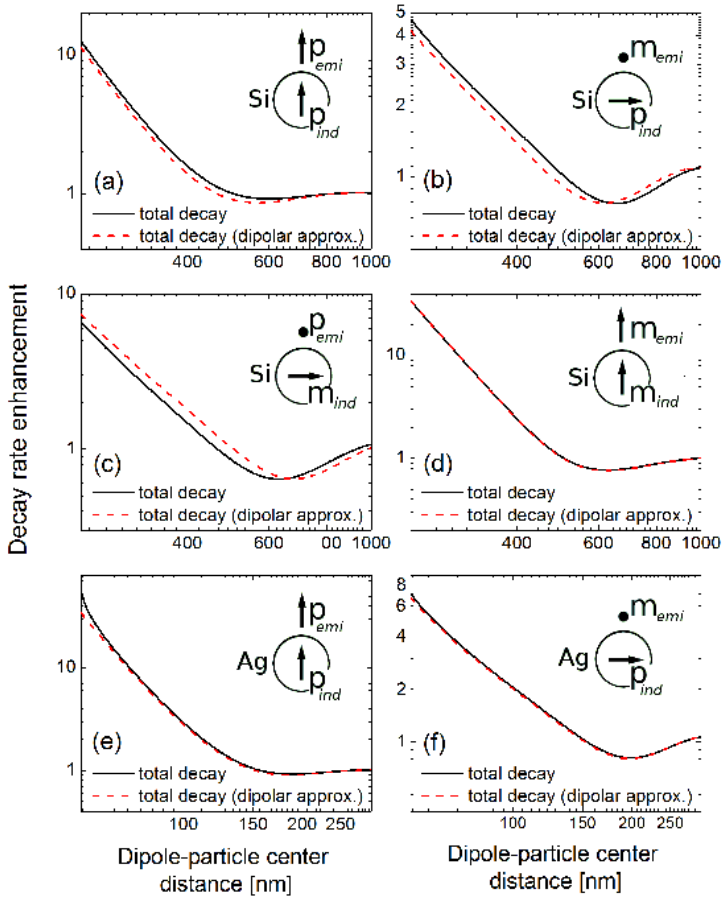

Fig. 5. Distance dependence of the decay rate enhancements calculated using the exact formulas (solid lines) and the dipolar interaction approach (dashed lines). In plots (a-d), the emitter is positioned near the 230 nm radius silicon sphere and for (e-f) - near the 50 nm radius silver sphere. The wavelength of radiation matches the dipolar electric mode at 1350 nm for silicon (a-b) and 420 nm for silver sphere (e-f) or the dipolar magnetic mode in silicon antenna at 1680 nm (c-d). In each case, only the dominant induced dipole is considered for the dipolar approximation, while the mode of the complementary nature (magnetic or electric) is neglected. The insets show the orientation and the electric of magnetic nature of both the emitter ($\mathbf{p}_{emi}$ or $\mathbf{m}_{emi}$, respectively) and the induced dipolar mode ($\mathbf{p}_{ind}$ or $\mathbf{m}_{ind}$, respectively) in the antenna. The distance is measured between the dipole and the center of the antenna.

#164420 - $15.00 USD Received 8 Mar 2012; revised 19 Apr 2012; accepted 26 Apr 2012; published 4 Jun 2012

the sphere: the magnetic emitter coupled to the silicon antenna at its electric dipolar resonance ($\lambda = 1350$ nm, Fig. 5(b)) and the electric emitter at the magnetic dipolar resonance ($\lambda = 1680$ nm, Fig. 5(c)).

For the silver antenna (Fig. 5(e)-5(f)), we show the distance dependence of the total decay rate enhancement for the radiation wavelength of 430 nm, which corresponds to the excitation of the dominant dipolar electric mode of the Ag particle. Almost perfect agreement between the exact solution and the results of the dipole-dipole interaction model is obtained both for the electric (Fig. 5(e)) and the magnetic emitter (Fig. 5(f)) oriented perpendicularly or parallelly to the surface of the antenna, respectively. The disagreements are mostly due to high order non-radiative contributions that become more significant for very short separation distances. However, we emphasize that the agreement between the simple model and the complete analytical solution is very good in all considered cases.

6. Conclusion

We have presented a detailed analysis of the radiative and non-radiative decay rates of a dipolar emitter positioned in the vicinity of a spherical particle. Based on Mie theory, we derived the general analytical expressions describing decay rates for both electric and magnetic dipole emitters. As we have shown, silicon nanospheres, with strong magnetic dipolar resonances in the near infrared, provide a canonical example of dielectric antennas that can be used to selectively enhance the magnetic dipolar emission. Interestingly, the resonant coupling between a dipolar (electric or magnetic) emitter and the dipolar Mie resonances is well described by a simple dipole-dipole interaction approach at certain wavelengths even when the emitter is in close proximity of the sphere surface.

Near the magnetic resonance, we found a strong enhancement of the decay rate of magnetic emitters which resembles the enhancement of electric dipole emission near a resonant plasmonic particle. However, while the total decay rate in plasmonic nano-antennas is often dominated by non-radiative channels, the total emission rate in loss-less silicon antennas is purely radiative. Our results show that nanosphere dielectric antennas are excellent platforms to enhance and manipulate magnetic dipolar emission with important possible applications as elements of infrared and telecommunication devices.

Appendix

Enhancements of the total and radiative decay rates of a magnetic dipolar emitter positioned in the vicinity of a sphere and fields distributions in the system

A formal derivation of a radiative and non-radiative decay rate enhancement is presented for a magnetic dipolar emitter $\mathbf{m}$ positioned at a location given by vector $\mathbf{r}'$ near a homogeneous sphere of radius a and dielectric function ε, embedded in a medium of dielectric function ε_e. The sphere is centered at the origin of the coordinate system. As previously, the radiation of the dipolar emitter will be characterized by a wavevector $k = 2\pi/\lambda\sqrt{\varepsilon_e}$, where λ denotes its vacuum radiation wavelength. The derivation is based on the work by Ruppin [9] in which the author considers an electric dipolar emitter positioned in the vicinity of a spherical particle.

The magnetic field of the magnetic dipolar emitter $\mathbf{m}$ can be expanded into a series of vector spherical harmonics $\mathbf{M}_\nu$ and $\mathbf{N}_\nu$ [23]

$$\mathbf{H}_{dip}(\mathbf{r},\omega) = \begin{cases} \sum_\nu D_\nu \left[p_\nu \mathbf{M}_\nu^{(1)}(k\mathbf{r}) + q_\nu \mathbf{N}_\nu^{(1)}(k\mathbf{r}) \right], & r > r' \\ \sum_\nu D_\nu \left[s_\nu \mathbf{M}_\nu^{(3)}(k\mathbf{r}) + t_\nu \mathbf{N}_\nu^{(3)}(k\mathbf{r}) \right], & r < r' \end{cases} \tag{16}$$

#164420 - $15.00 USD Received 8 Mar 2012; revised 19 Apr 2012; accepted 26 Apr 2012; published 4 Jun 2012

where the summation is performed over indices

$$\sum_{\nu} = \sum_{\sigma=o,e} \sum_{n=1}^{\infty} \sum_{m=0}^{n}, \tag{17}$$

with

$$D_{\nu} = \delta_m \frac{(2n+1)(n-m)!}{4n(n+1)(n+m)!} \tag{18}$$

and

$$\delta_m = \begin{cases} 1, & m = 0 \\ 2, & m > 0. \end{cases} \tag{19}$$

The expansion coefficients are given by

$$s_{\nu} = \frac{ik^3}{\pi} \mathbf{M}_{\nu}^{(1)}(k\mathbf{r}') \cdot \mathbf{m} \tag{20}$$

$$t_{\nu} = \frac{ik^3}{\pi} \mathbf{N}_{\nu}^{(1)}(k\mathbf{r}') \cdot \mathbf{m} \tag{21}$$

$$p_{\nu} = \frac{ik^3}{\pi} \mathbf{M}_{\nu}^{(3)}(k\mathbf{r}') \cdot \mathbf{m} \tag{22}$$

$$q_{\nu} = \frac{ik^3}{\pi} \mathbf{N}_{\nu}^{(3)}(k\mathbf{r}') \cdot \mathbf{m}. \tag{23}$$

The above expansion and its coefficients can be derived by a transformation

$$\mathbf{E} = -Z\mathbf{H}_p, \mathbf{H} = \frac{1}{Z}\mathbf{E}_p \tag{24}$$

where $\mathbf{E}_p$ and $\mathbf{H}_p$ are, respectively, the electric and magnetic fields of an electric dipole $\mathbf{p}$, as given by Ruppin [9], with the substitution $\mathbf{p} \to \mathbf{m}/c$ [28]. Z is the impedance of the medium and c - the speed of light in the medium.

The scattered field and the field inside the sphere are expanded in a similar manner

$$\mathbf{H}_{sc}(\mathbf{r}, \omega) = \sum_{\nu} D_{\nu} \left[u_{\nu} \mathbf{M}_{\nu}^{(3)}(k\mathbf{r}) + v_{\nu} \mathbf{N}_{\nu}^{(3)}(k\mathbf{r}) \right] \tag{25}$$

$$\mathbf{H}_{tr}(\mathbf{r}, \omega) = \sum_{\nu} D_{\nu} \left[f_{\nu} \mathbf{M}_{\nu}^{(1)}(k_1\mathbf{r}) + g_{\nu} \mathbf{N}_{\nu}^{(1)}(k_1\mathbf{r}) \right] \tag{26}$$

where

$$k_1 = 2\pi/\lambda\sqrt{\varepsilon}. \tag{27}$$

Since our goal is to calculate both the radiated power and the power dissipated inside a sphere (for a non-vanishing imaginary part of the dielectric function ε), we need to derive the expansion coefficients: $u_{\nu}, v_{\nu}, f_{\nu}, g_{\nu}$ by considering the boundary conditions at the surface of sphere:

$$\hat{\mathbf{r}} \times (\mathbf{H}_{dip} + \mathbf{H}_{sc}) = \hat{\mathbf{r}} \times \mathbf{H}_{tr} \tag{28}$$

$$\hat{\mathbf{r}} \times (\mathbf{E}_{dip} + \mathbf{E}_{sc}) = \hat{\mathbf{r}} \times \mathbf{E}_{tr} \tag{29}$$

where $\hat{\mathbf{r}}$ is a unitary radial vector.
The electric fields $\mathbf{E}_{dip}$, $\mathbf{E}_{sc}$ and $\mathbf{E}_{tr}$ of the magnetic dipole can be calculated using a relation

$$\mathbf{E}_{dip} = \frac{i}{\omega\varepsilon_0\varepsilon_e} \nabla \times \mathbf{H}_{dip} \tag{30}$$

#164420 - $15.00 USD Received 8 Mar 2012; revised 19 Apr 2012; accepted 26 Apr 2012; published 4 Jun 2012

and the properties of spherical vector wave functions

$$k'\mathbf{M}_\nu(k'\mathbf{r}) = \nabla \times \mathbf{N}_\nu(k'\mathbf{r}) \tag{31}$$

$$k'\mathbf{N}_\nu(k'\mathbf{r}) = \nabla \times \mathbf{M}_\nu(k'\mathbf{r}) \tag{32}$$

Using the expansions of the magnetic field in Eqs. (16), (25), (26) and the corresponding electric field expansions given by Eq. (30), we obtain from the boundary conditions in Eqs. (28) and (29) the following relations:

$$u_\nu = -a_n p_\nu \tag{33}$$

$$v_\nu = -b_n q_\nu \tag{34}$$

$$f_\nu = -\alpha_n p_\nu \tag{35}$$

$$g_\nu = -\beta_n q_\nu \tag{36}$$

where a_n and b_n are the Mie coefficients given by Eqs. (9) and (10). The coefficients for the transmitted fields α_n and β_n are defined as

$$\alpha_n = \frac{\psi'(ka)\zeta(ka) - \psi(ka)\zeta(ka)'}{\psi(k_1 a)\zeta'(ka) - \psi'(k_1 a)\zeta(ka)/M} \tag{37}$$

$$\beta_n = \frac{\psi(ka)\zeta(ka)' - \psi'(ka)\zeta(ka)}{\psi'(k_1 a)\zeta(ka) - \psi(k_1 a)\zeta'(ka)/M} \tag{38}$$

where $k_1 = k\sqrt{\varepsilon/\varepsilon_e} = kM$. Note that we adopt here the definitions of the Mie coefficients by Bohren and Huffman [23], which differ from those used by Ruppin [9] and - more recently - Mertens et al. [12] by interchanging $a_n \leftrightarrow -b_n$ and $\alpha_n \leftrightarrow -\beta_n$.

Evaluating the Poynting vector of the incident and scattered fields and integrating its flux over a very large sphere we obtain the power radiated from the system

$$W_{RAD} = \sqrt{\frac{\varepsilon_0}{\mu_0}}\frac{\pi}{k^2}\sum_\nu \delta_m \frac{(2n+1)(n-m)!}{8n(n+1)(n+m)!}\left[|s_\nu + u_\nu|^2 + |t_\nu + v_\nu|^2\right] \tag{39}$$

The rate of the energy dissipation is given by

$$W_{NON-RAD} = \frac{1}{2}\int_{sphere} \kappa |\mathbf{E}_{tr}(\mathbf{r})|^2 d\mathbf{r} \tag{40}$$

where $\kappa = \omega\Im(\varepsilon)$ is the conductivity of the sphere. Substituting into the above expressions the expansion coefficients $s_\nu, t_\nu, p_\nu, q_\nu$ given by Eqs. (20)-(23), and normalizing the results to the power radiated by a unitary quantum efficiency dipole in the homogeneous medium, we obtain the radiative and total decay rate enhancements of the magnetic dipole (Eqs. (5)-(8)). It should be noted that the evaluation of these quantities requires notably fewer spherical harmonics to be calculated in comparison to an exact description of the strongly inhomogeneous near fields induced in the proximity of the sphere.

We note that our expressions are consistent with those introduced by quantum mechanical considerations of the magnetic dipolar transition between two states of the molecule in the vicinity of a lossless spherical nanoparticle [22].

#164420 - $15.00 USD Received 8 Mar 2012; revised 19 Apr 2012; accepted 26 Apr 2012; published 4 Jun 2012

Acknowledgments

Financial support from the ETORTEK 2011 "nanoiker" of the Department of the Industry of the Basque Country Government, the WELCOME program "Hybrid nanostructures as a stepping-stone towards efficient artificial photosynthesis" awarded by the Foundation for Polish Science, the Spanish MEC FIS2010-19609-C02-02, Consolider NanoLight (CSD2007-00046) and FIS2009-13430-C02 research grants and the Comunidad de Madrid Microseres-CM Program (S2009/TIC- 1476) are gratefully acknowledged. RE and JA acknowledge support from the Spanish National project Euroinvestigación EUI200803816 CUBiHOLE.

#164420 - $15.00 USD Received 8 Mar 2012; revised 19 Apr 2012; accepted 26 Apr 2012; published 4 Jun 2012